Supplementary Information

Gadolinium oxide-decorated graphene oxide-based dual-stimuli-responsive smart fluids

Hyukjoon Gwon, Hamin Kim and Seungae Lee*

Department of Chemical Engineering, Konkuk University, 120 Neungdong-ro, Gwangjin-gu, Seoul 05029, Republic of Korea

* Corresponding author. Tel.: +82-2-2049-6109; E-mail address: salee@konkuk.ac.kr (S. Lee).

Supplementary Information

1. High resolution TEM images of GO and Gd_2O_3/GO composite.

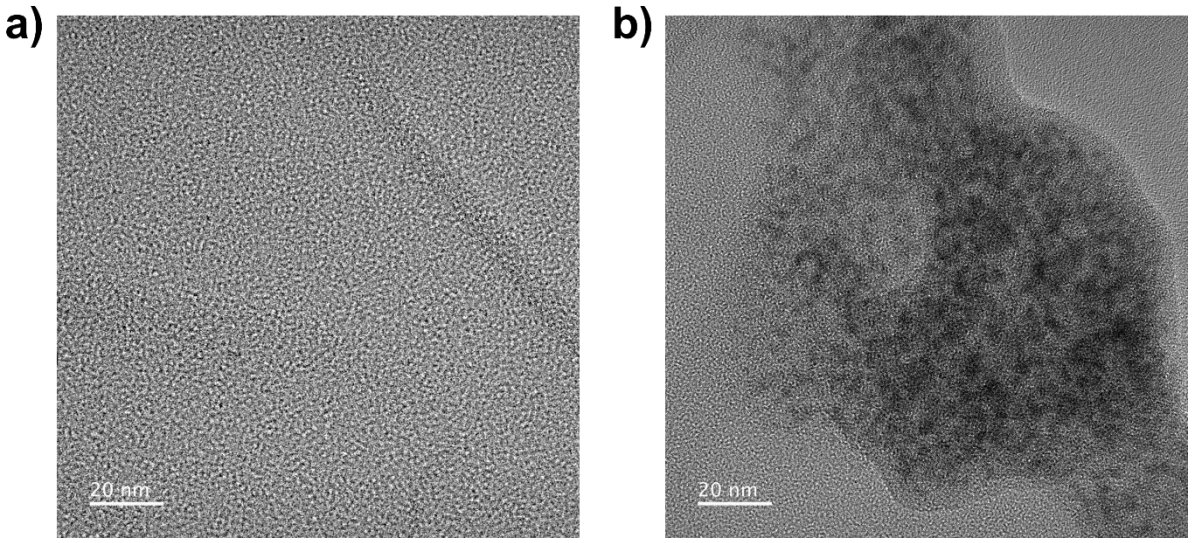

Fig. S1 High resolution TEM images of a) GO and b) Gd_2O_3/GO composite with a Gd_2O_3:GO ratio of 1:2.

2. C 1s, O 1s and Gd 4d XPS spectra of Gd_2O_3/GO composite with Gd_2O_3:GO ratios of 1:2 and 1:3.

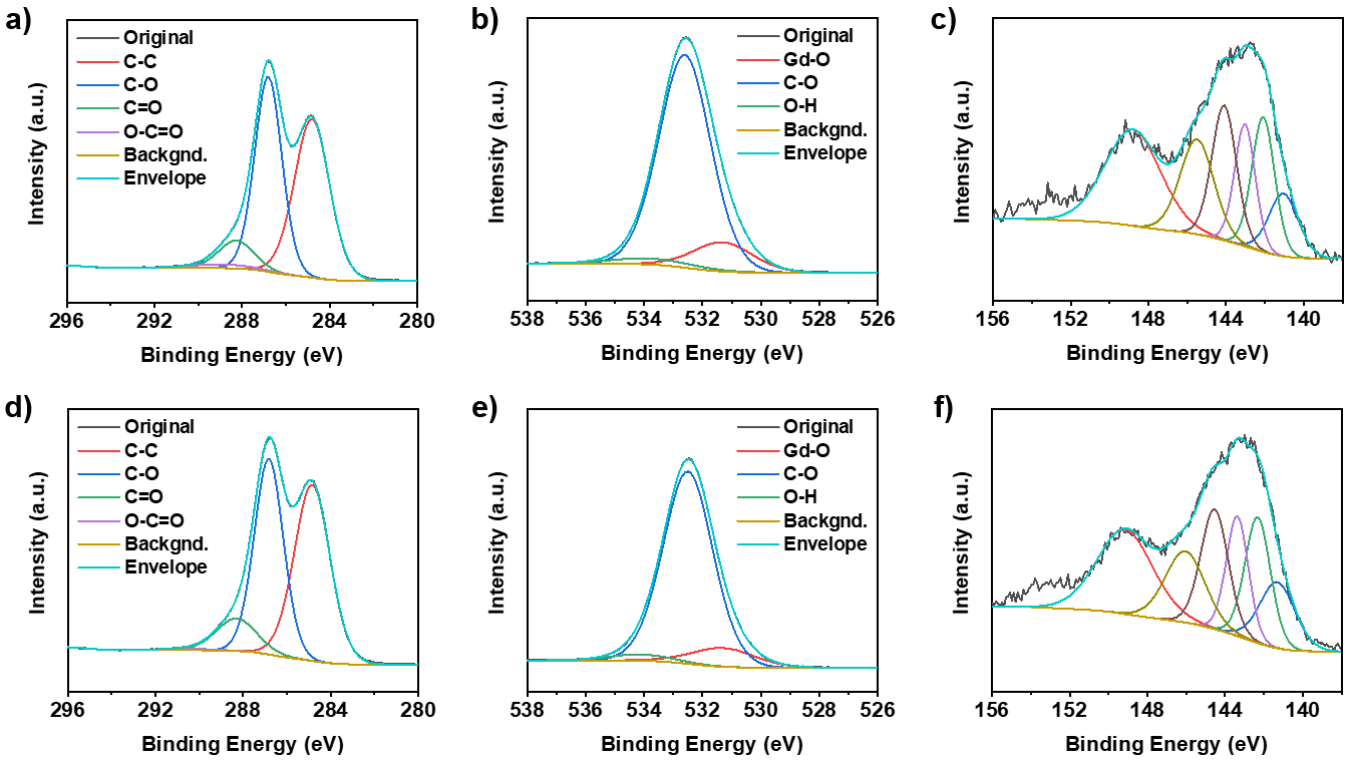

Fig. S2 a) C 1s, b) O 1s and c) Gd 4d XPS spectra of the Gd_2O_3/GO composite with a Gd_2O_3:GO ratio of 1:2, and d) C 1s, e) O 1s and f) Gd 4d XPS spectra of the Gd_2O_3/GO composite with a Gd_2O_3:GO ratio of 1:3.

3. FTIR spectra of GO and Gd_2O_3/GO composites.

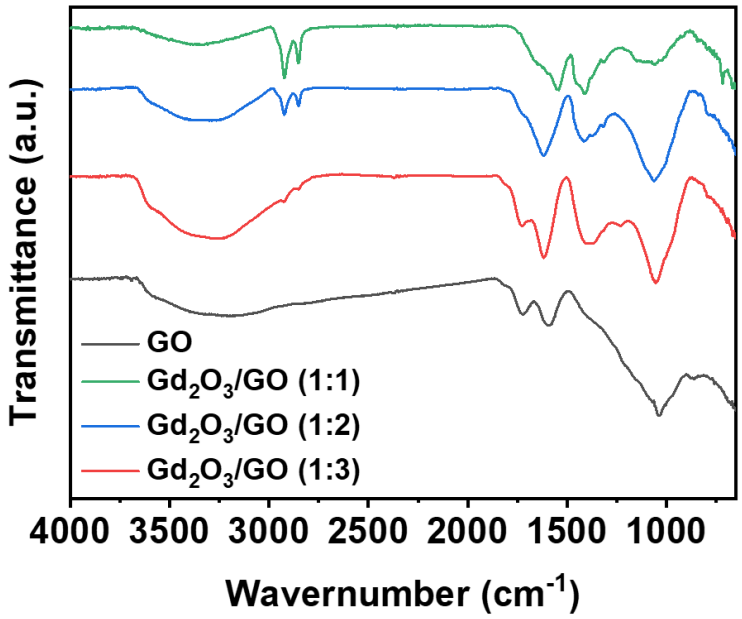

Fig. S3 FTIR spectra of GO and Gd_2O_3/GO composites with Gd_2O_3:GO ratios of 1:1, 1:2, and 1:3.

4. Fitting results and parameters for Bingham model and CCJ model of Gd_2O_3/GO-based EMR fluids.

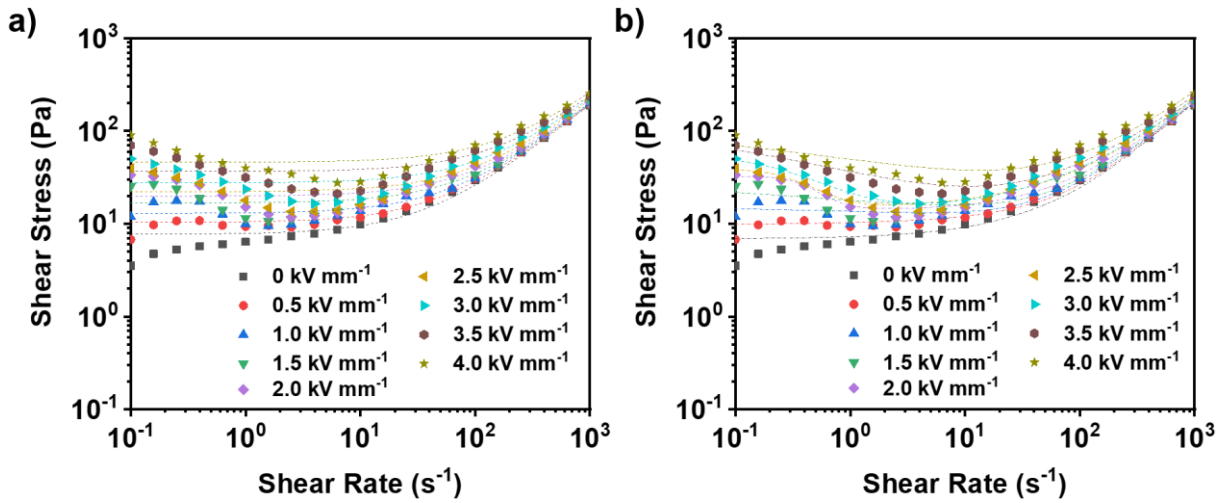

Fig. S4 Electro-responsive properties of the Gd_2O_3/GO-based EMR fluids with a Gd_2O_3:GO ratio of 1:1 and fitted results for a) Bingham model and b) CCJ model.

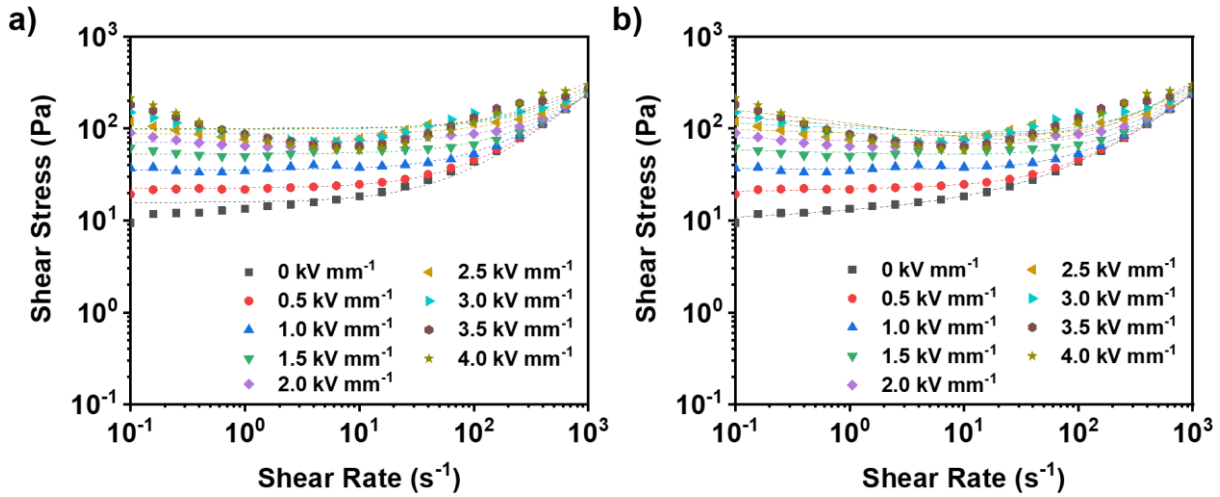

Fig. S5 Electro-responsive properties of the Gd_2O_3/GO-based EMR fluids with a Gd_2O_3:GO ratio of 1:2 and fitted results for a) Bingham model and b) CCJ model.

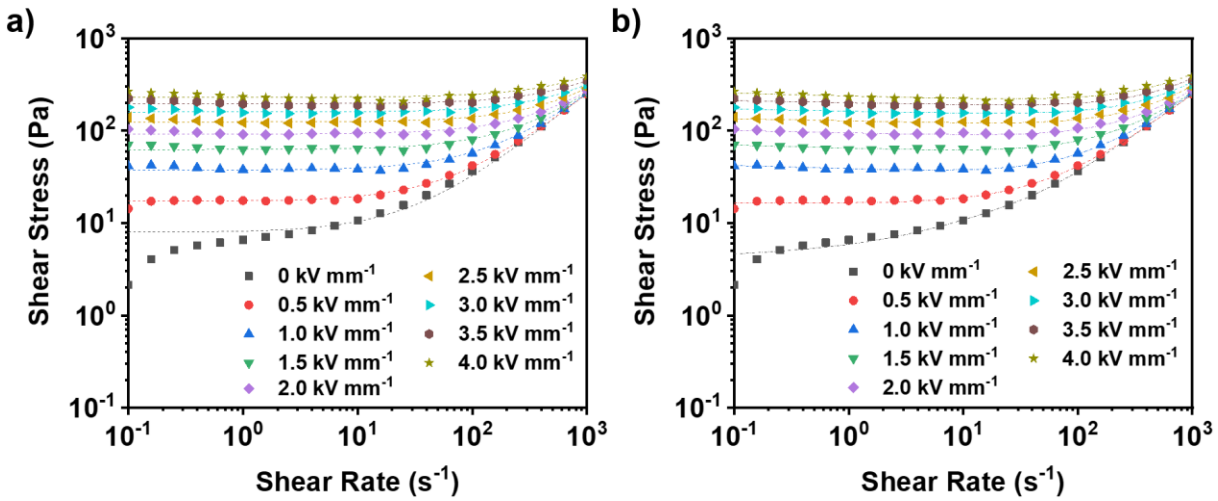

Fig. S6 Electro-responsive properties of the Gd_2O_3/GO-based EMR fluids with a Gd_2O_3:GO ratio of 1:3 and fitted results for a) Bingham model and b) CCJ model.

Table S1. The fitting parameters of the Bingham and Cho–Choi–Jhon (CCJ) models for the flow curves of the Gd_2O_3/GO composite-based EMR fluid with a Gd_2O_3:GO ratio of 1:1.

Model	Parameter[a]	0 kV mm^{-1}	0.5 kV mm^{-1}	1.0 kV mm^{-1}	1.5 kV mm^{-1}	2.0 kV mm^{-1}	2.5 kV mm^{-1}	3.0 kV mm^{-1}	3.5 kV mm^{-1}	4.0 kV mm^{-1}
Bingham	τ_y	7.682	10.31	12.90	16.69	19.74	22.11	27.55	36.50	45.98
	η_∞	0.185	0.184	0.186	0.181	0.183	0.193	0.199	0.205	0.217
CCJ	τ_y	6.143	8.506	13.63	43.43	18.58	27.55	48.66	120.4	138.1
	η_∞	0.188	0.191	0.197	0.195	0.201	0.213	0.222	0.234	0.252
	t_1	0.005	0.007	0.008	12.75	2.116	2.593	3.076	13.65	8.542
	t_2	0.187	0.105	0.113	3.523	0.014	0.007	0.040	0.013	0.018
	α	1.862	1.347	0.391	0.165	3.271	2.122	1.230	0.448	0.286
	β	0.906	0.926	0.985	1	1	0.935	0.882	0.689	0.525

[a] τ_y: yield stress / η_∞: viscosity at high shear rate / t_1, t_2: time constant / α, β: exponents for model fitting.

Table S2. The fitting parameters of the Bingham and Cho–Choi–Jhon (CCJ) models for the flow curves of the Gd_2O_3/GO composite-based EMR fluid with a Gd_2O_3:GO ratio of 1:2.

Model	Parameter[a]	0 kV mm^{-1}	0.5 kV mm^{-1}	1.0 kV mm^{-1}	1.5 kV mm^{-1}	2.0 kV mm^{-1}	2.5 kV mm^{-1}	3.0 kV mm^{-1}	3.5 kV mm^{-1}	4.0 kV mm^{-1}
Bingham	τ_y	15.72	22.44	35.28	52.75	71.19	87.35	98.45	100.2	99.25
	η_∞	0.226	0.220	0.202	0.183	0.166	0.158	0.167	0.193	0.223
CCJ	τ_y	7.85	18.40	71.80	94.72	121.1	193.3	220.7	265.3	314.4
	η_∞	0.235	0.240	0.239	0.243	0.245	0.248	0.259	0.272	0.294
	t_1	0.022	0.034	1.828	0.014	0.010	5.362	8.418	10.51	17.33
	t_2	0.012	0.025	7.382	8.925	9.514	1.901	0.011	0.005	0.019
	α	0.309	0.642	0.026	0.071	0.092	0.068	0.128	0.181	0.251
	β	0.768	0.715	0.388	0.987	0.996	1	0.762	0.522	0.315

[a] τ_y: yield stress / η_∞: viscosity at high shear rate / t_1, t_2: time constant / α, β: exponents for model fitting.

Table S3. The fitting parameters of the Bingham and Cho–Choi–Jhon (CCJ) models for the flow curves of the Gd_2O_3/GO composite-based EMR fluid with a Gd_2O_3:GO ratio of 1:3.

Model	Parameter[a]	0 kV mm^{-1}	0.5 kV mm^{-1}	1.0 kV mm^{-1}	1.5 kV mm^{-1}	2.0 kV mm^{-1}	2.5 kV mm^{-1}	3.0 kV mm^{-1}	3.5 kV mm^{-1}	4.0 kV mm^{-1}
Bingham	τ_y	7.915	17.18	37.31	62.46	92.16	124.3	159.0	195.9	230.9
	η_∞	0.249	0.234	0.214	0.195	0.175	0.165	0.158	0.154	0.162
CCJ	τ_y	4.132	31.45	62.94	138.7	170.5	223.0	313.2	383.0	496.0
	η_∞	0.250	0.249	0.254	0.263	0.271	0.291	0.316	0.345	0.387
	t_1	0.027	0.031	0.005	9.931	0.343	0.017	0.860	8.101	6.017
	t_2	0.016	3.841	6.511	0.166	0.030	0.335	0.038	0.003	0.001
	α	2.037	0.013	0.099	0.067	0.059	0.060	0.049	0.049	0.072
	β	0.496	0.215	0.2153	0.545	1	1	1	1	0.711

[a] τ_y: yield stress / η_∞: viscosity at high shear rate / t_1, t_2: time constant / α, β: exponents for model fitting.

5. Comparative analysis of GO and Fe_3O_4-based smart fluids.

Table S4. Comparative analysis of ER, MR and EMR fluids composed of GO and Fe_3O_4-based materials.

Stimuli	Stimuli-responsive material	Filler content	Maximum applicable field strength/stimuli response ($0.1\ s^{-1}$)[a]	Reference
Electric field	GO	5 wt%	5.0 kV mm^{-1} / ~280 Pa	1
	GO	5 wt%	2.5 kV mm^{-1} / ~200 Pa	2
	Polyhedral oligomeric silsesquioxane-decorated GO	3 wt%	3.0 kV mm^{-1} / ~400 Pa	3
	PS–GO microspheres	10 vol%	2.0 kV mm^{-1} / ~100 Pa	4
	GO/Al_2O_3 composite	20 wt%	5.0 kV mm^{-1} / ~100 Pa	5
	Graphene oxide-coated mesoporous silica spheres	3 wt%	3.0 kV mm^{-1} / ~35 Pa	6
Magnetic field	Octahedral-shaped Fe_3O_4 nanoparticles	10 vol%	343 kA m^{-1} / ~1000 Pa	7
	Flower-like Fe_3O_4 microspheres	30 wt%	250 kA m^{-1} / ~20 Pa	8
	Fe_3O_4@mSiO_2 nanoparticles	5 vol%	171 kA m^{-1} / ~1000 Pa	9
	Core–shell structured PS/Fe_3O_4 microbead	11 vol%	343 kA m^{-1} / ~80 Pa	10
	Carbon layer modified Fe_3O_4 nanospheres	10 wt%	350 kA m^{-1} / ~10 Pa	11
	PMMA/ Fe_3O_4 composites	10 vol%	1999 mA / ~40 Pa	12
Electric field & Magnetic field	Fe_3O_4@GO-PS composites	5 vol% (ER) / 10 vol% (MR)	E: 3.0 kV mm^{-1} / ~25 Pa M: 171 kA m^{-1} / ~15 Pa	13
	Fe_3O_4/GO composites	15 wt% (ER) / 20 vol% (MR)	E: 2.5 kV mm^{-1} / ~90 Pa M: 257 kA m^{-1} / ~650 Pa	14
	SiO_2/TiO_2@ Fe_3O_4/SiO_2 nanoparticles	20 vol%	E: 3.0 kV mm^{-1} / ~10 Pa M: 796 kA m^{-1} / ~350 Pa	15
	Gd_2O_3/GO composite	0.6 wt%	E: 4.0 kV mm^{-1} / 266 Pa M: 343 kA m^{-1} / 1416 Pa	This work

[a] E: maximum applied electric field, M: maximum applied magnetic field.

6. References.

1 J. Hong and J. Jang, *Soft Matter*, 2012, **8**, 7348–7350.

2 W. Zhan, Y. Liu, H. Choi and S. Kim, *ACS Appl. Mater. Interfaces*, 2012, **4**, 2267–2272.

3 Y. Li, Y. Guan, Y. Liu, J. Yin and X. Zhao, *Nanotechnology*, 2016, **27**, 195702.

4 S. Kim, W. Zhang and H. Choi, *J. Mater. Chem. C*, 2014, **2**, 7541–7546.

5 W. Zhang, H. Choi and Y. Leong, *Mater. Chem. Phys.*, 2014, **145**, 151–155.

6 C. Yoon, S. Lee, S. Hong and J. Jang, *J. Colloid Interface Sci.*, 2015, **438**, 14–21.

7 H. Jung and H. Choi, *J. Appl. Phys.*, 2015, **117**, 17E708.

8 G. Wang, D. Zhao, N. Li, Y. Zeng, S. Han, Y. Ma, X. Dong and R. Yu, *J. Ind. Eng. Chem.*, 2019, **79**, 17–225.

9 W. Han, S. Piao, H. Choi and Y. Seo, *Colloids Surf. A: Physicochem. Eng. Asp.*, 2017, **524**, 79–86.

10 F. Fang, J. Kim and H. Choi, *Polymer*, 2009, **50**, 2290–2293.

11 L. Bai, L. Pei, S. Cao, X. He, M. Sang, W. Jiang, S. Xuan and X. Gong, *J. Magn. Magn. Mater.*, 2020, **505**, 166734.

12 M. Hong, B. Park and H. Choi, *J. Phys. Conf. Ser.*, 2009, **149**, 012055.

13 Q. Lu, H. Jin and H. Choi, *J. Mol. Liq.*, 2022, **365**, 120083.

14 W. Zhang, Y. Tian, Y. Liu, Z. Song, J. Liu and H. Choi, *RSC Adv.*, 2016, **6**, 77925–77930.

15 C. Yoon, Y. Jang, S. Lee and J. Jang, *J. Mater. Chem. C*, 2018, **6**, 10241–10249.